

# Dimerization process and elementary excitations in spin-Peierls chains coupled by frustrated interactions

D Mastrogiuseppe, C Gazza and A Dobry

Facultad de Ciencias Exactas Ingeniería y Agrimensura, Universidad Nacional de Rosario and Instituto de Física Rosario, Bv. 27 de Febrero 210 bis, 2000 Rosario, Argentina.

E-mail: dmastro@ifir.edu.ar

**Abstract.** We consider the ground state and the elementary excitations of an array of spin-Peierls chains coupled by elastic and magnetic interactions. It is expected that the effect of the magnetic interchain coupling will be to reduce the dimerization amplitude and that of the elastic coupling will be to confine the spin one-half solitons corresponding to each isolated chain. We show that this is the case when these interactions are not frustrated. On the other hand, in the frustrated case we show that the amplitude of dimerization in the ground state is independent of the strength of the interchain magnetic interaction in a broad range of values of this parameter. We also show that free solitons could be the elementary excitations when only nearest neighbour interactions are considered. The case of an elastic interchain coupling is analyzed on a general energetic consideration. To study the effect of the magnetic interchain interaction the problem is simplified to a two-leg ladder which is solved using density matrix renormalization group (DMRG) calculations. We show that the deconfinement mechanism is effective even with a significantly strong antiferromagnetic interchain coupling.

PACS numbers: 75.10.Jm, 75.10.Pq, 75.40.Mg

Elementary excitations of antiferromagnetic systems are spin-one magnons which are bosonic in character and correspond to flipping locally the spin of one electron. They give rise to a definite peak in the dynamical structure factor which is observed in neutron scattering measurements. In a one-dimensional antiferromagnet, this picture breaks down and the concept of fractionalized excitation has been proposed in the last years to explain the excitation spectra. The excitation spectrum of a 1D antiferromagnetic Heisenberg model is a paradigmatic example of a fractional quantum state. The elementary excitations are spin- $\frac{1}{2}$  spinons which are topological excitations identified as quantum domain walls. The spectral signal corresponding to the excitation of two spinons shows a highly dispersive continuum without a definite one-particle peak in the dynamic susceptibility. Measurements of the two-spinon continuum have been achieved in the quasi-one-dimensional antiferromagnetic system  $\text{KCuF}_3$  [1]. Since the discovery of the cuprate superconductors an intense activity has been carried out to

see if a fractional quantum state is possible in a two-dimensional antiferromagnet. An experimental realization seems to be found in  $\text{Cs}_2\text{CuCl}_4$  [2].

Some analogies appear in the excitation spectra when the magnetism is coupled to phonons in the so-called spin-Peierls systems. This coupling leads to a magneto-structural transition towards a dimerized low-temperature phase, opening a gap in the magnetic spectra. Even though the excitation spectrum of an isolated spin-phonon chain is not exactly known, an early semiclassical analysis of a bosonized field theory [3] gives some insight to this problem. The elementary excitation is a soliton, a topological defect which separates two different phases of the dimerized order. It is a mixed magnetic and structural excitation carrying a spin- $\frac{1}{2}$ . Therefore, the dynamical response of a pure spin-phonon system should be dominated by a two-soliton continuum above the spin gap. Numerical calculations in small chains confirm this scenario [4].

The role of the interchain coupling should be taken into account for application to a real compound. It was particularly analyzed in connection with neutron and optical spectra measurements in the inorganic spin-Peierls system  $\text{CuGeO}_3$  [5, 6]. It has been concluded that solitons are always confined by the interchain coupling. It means that no trace of solitons is present in the excitation spectrum. Different routes have been followed to analyze the effect of the interchain coupling. In one of them a linear confinement potential between the solitons has been considered as a result of a mean field treatment of the interchain coupling [5]. A ladder of bound soliton-antisoliton states appears before a magnon continuum. In other approach [6], a mixed lattice and magnetic excitation called *domain* was found in a semiclassical approximation of the bosonized theory of the two-dimensional spin-phonon system. The domain is a triplet excitation. Excitations inside the domain give rise to a series of states before the appearance of a two-domain continuum. Experiments in  $\text{CuGeO}_3$  [9] have shown the existence of a peak separated from a continuum, in consistency with the previous pictures. The peak could be associated with a magnon excitation and the continuum with a two-magnon continuum.

We note that by integrating out the phonon coordinates the adiabatic-antiadiabatic crossover has been studied in the one-dimensional model [8]. Moreover, the dynamic correlation function has been studied in the antiadiabatic limit for the problem of coupled chains [7]. The effective one-chain problem has been solved by using exact results from the sine-Gordon theory corresponding to the continuum limit of the effective magnetic problem. The interchain interactions have been taken into account by a RPA approach. The dynamic susceptibility has also a peak corresponding to a spin-1 excitation (which we call a magnon) and a continuum.

Now the question arises about if free solitons could be observed in a real system. That is to say, if it is possible to observe a two-soliton continuum above the gap in a spin-Peierls material. The complete answer to this question is a formidable problem because it implies the calculation of the dynamic spin-spin correlation function for a coupled 2D or 3D spin-phonon problem. As a first step we use a semiclassical approach in the present work. Our purpose is to show that a frustrated nearest neighbour interchain

coupling in a quasi-one-dimensional spin-Peierls system does not confine the in-chain solitons.

Our work is also motivated by the recently identified materials TiOCl and TiOBr as spin-Peierls compounds [10]. These materials deviate from a canonical spin-Peierls behaviour due to the existence of an intermediate incommensurate phase (between the uniform and dimer phases). It has been shown that a frustrated interchain coupling in the bi-layer structure could be the origin of that incommensurate phase [11]. Therefore we propose as a minimal model for this material a set of antiferromagnetic spin-Peierls chains coupled by a frustrated magneto-elastic interaction. The result of the present paper could be taken as a starting point to interpret the magnetic excitation spectra in the low-temperature phases of these materials.

Aiming to discuss the previous posed problem, in this work we compare two different models for the interchain coupling. In both models an array of one-dimensional Heisenberg chains coupled to the lattice deformation is described by the following Hamiltonian:

$$H_{in} = \sum_{i,j} \frac{(P_i^j)^2}{2m} + \frac{1}{2} K_{in} \sum_{i,j} (u_{i+1}^j - u_i^j)^2 + J_{in} \sum_{i,j} [1 + \alpha(u_{i+1}^j - u_i^j)] \mathbf{S}_i^j \cdot \mathbf{S}_{i+1}^j \quad (1)$$

where we denote by  $i$  the site of the  $j$ th chain, and the 'in' subscript indicates that this part of the Hamiltonian takes into account only the in-chain interactions.  $\mathbf{S}_i^j$  are spin- $\frac{1}{2}$  operators with exchange constant  $J_{in}$  along the x-axis of a non-deformed underlying lattice. In our simplified model we took the scalar ionic coordinates  $u_i^j$  to be the relevant for the dimerization process and  $P_i^j$  are their conjugate momenta.  $K_{in}$  is the elastic coupling along the chain. Furthermore  $\alpha$  measures the deformation effect on the magnetic exchange constant.

The two cases we compare are differentiated by the interchain coupling configuration. In the first one, the magnetic sites lay on a lattice with square geometry. The interchain coupling reads:

$$H_{inter}^{sq} = \frac{1}{2} K_{inter} \sum_{i,j} (u_i^{j+1} - u_i^j)^2 + J_{inter} \sum_{i,j} \mathbf{S}_i^j \cdot \mathbf{S}_i^{j+1} \quad (2)$$

In the other case they reside on an underlying triangular lattice. Equation (2) changes to:

$$H_{inter}^{tr} = \frac{1}{2} K_{inter} \sum_{i,j} [(u_i^{j+1} - u_i^j)^2 + (u_{i+1}^{j-1} - u_i^j)^2] + J_{inter} \sum_{i,j} (\mathbf{S}_i^j \cdot \mathbf{S}_i^{j+1} + \mathbf{S}_i^j \cdot \mathbf{S}_{i+1}^{j-1}) \quad (3)$$

where  $K_{inter}$  and  $J_{inter}$  are the elastic and magnetic interchain coupling constants. We have considered only nearest neighbour interactions in both cases. We finally get the complete Hamiltonian as follows:

$$H = H_{\text{in}} + H_{\text{inter}} \quad (4)$$

where we must replace the second term of the sum with equation (2) or (3) depending on the case.

Let us begin with a qualitative energetic interpretation in order to describe the ground state and the elementary excitations of these systems. We treat the problem in the adiabatic approximation, i.e. we consider the ionic coordinates as classical static variables and neglect the kinetic term in (1). It is known that the one-dimensional spin-phonon model given by (1) dimerizes as the result of a competition between the elastic and magnetic interactions. In figure 1 we show the array of dimerized chains (horizontally positioned) in the square geometry.

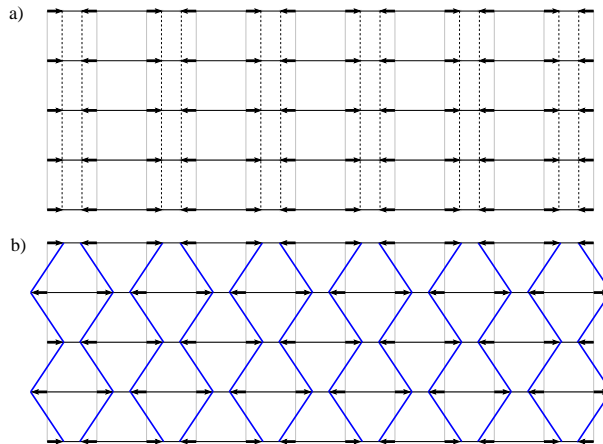


**Figure 1.** Schematic representation of the dimerized phase in the square lattice (gray background) for (a) the in-phase and (b) an out-of-phase configuration. Arrows signal the displacement of the atoms. The thin dashed lines correspond to unperturbed interchain springs and the blue continuous ones forming zigzag paths are dilated springs.

Each spin belongs to a singlet and we therefore assume that  $J_{\text{inter}}$  is not active (at least for a small enough value of  $J_{\text{inter}}$ , see the analysis for ladders below). Therefore, we are not going to consider its effects in the present analysis. In this figure we represent two possible configurations of dimerized chains. In the upper graphic, each chain is in phase with its neighboring chains, i.e. the  $i$ th ion of chain  $j$  moves in the same direction of the  $i$ th ion in chains  $j + 1$  and  $j - 1$ . In this case we can observe that this in-phase configuration does not cost additional interchain elastic energy because every interchain spring is unperturbed. The lower part of the figure shows a possible out-of-phase configuration where the  $i$ th ion of chain  $j$  moves in opposite direction to that of the  $i$ th ion of chains  $j + 1$  and  $j - 1$ . Here, there is an additional energy cost due to the expansion of every interchain spring. Any other possible out-of-phase configuration will also have perturbed interchain springs so the in-phase configuration is the only one that minimizes the total energy.

Now let us see what happens in the triangular geometry. Again, in figure 2 we show two possible arrangements, the in-phase one in the upper part of the figure and an out-of-phase configuration (where dimers in next-nearest neighbour chains are mutually out of phase) in the lower part.

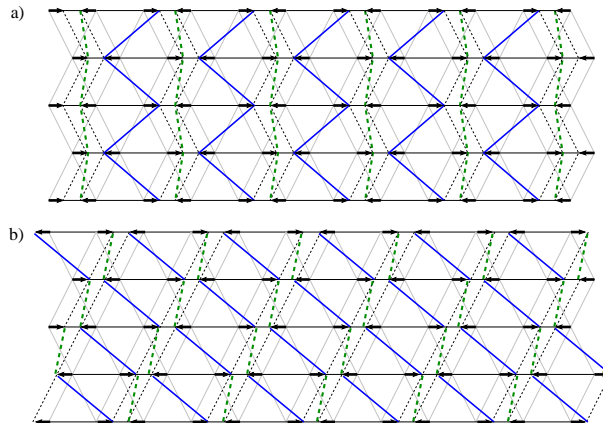


**Figure 2.** Schematic representation of the dimerized phase in the triangular lattice (gray background) for (a) the in-phase arrangement and (b) an out-of-phase configuration. The thin dashed lines correspond to unperturbed interchain springs, the thick blue continuous (green dashed) ones forming zigzag paths are dilated (compressed) springs.

In this figure we can observe that there is alternately a compressed spring, an unperturbed one, a dilated one and then another unperturbed spring. Here we have the first difference with respect to the square geometry: meanwhile in the square geometry there is no additional elastic energy cost in the dimerization process, in the triangular one there are always deformed interchain springs. The second difference arises when comparing the two panels of figure 2 where we observe that in both cases we have the same deformation pattern of interchain springs, i.e. due to the frustrated configuration of the model the lower energy state of the system is degenerate with a degeneracy that depends on all the possible combinations of dimerization patterns. Note that if there were next-nearest neighbour interactions in the model, the system would lock next-nearest neighbour chains in phase but there is still no restriction with respect to nearest neighbour chains.

Now let us include solitons as point defects dephasing the dimerization order in the in-phase arrangements of figures 1 and 2. We include two of such defects in the same chain, and therefore the situation could be represented as shown in figure 3. Note the essential difference in both cases, for the square lattice the intermediate zone dimerizes in antiphase to the background. The energy cost of this configuration is proportional to the distance between the solitons, so they are always confined with a linear confining potential. In the triangular geometry this situation does not take place because the interchain energy does not depend on the relative dimerization phase of two nearest neighbour chains and the only additional energy respect to the dimerized state

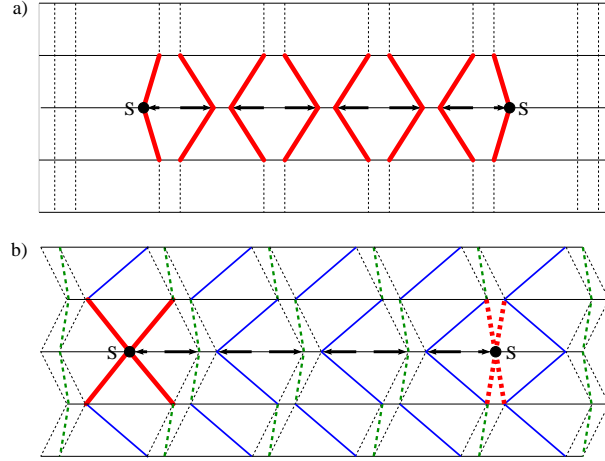


**Figure 3.** Schematic representation of the dimerized phase including two solitons (signalled by an S) in the central chain for (a) square and (b) triangular lattices. The thick red lines show the perturbation induced by the excitations on the interchain springs. Note that in (a) every intersoliton spring is affected and in (b) the excitations produce a local perturbation with respect to the dimerized configuration.

is the local cost to create the solitons. This means that the solitons are not interacting excitations in the triangular geometry.

The previous analysis could be checked quantitatively by the following construction. As both the lattice dimerization and soliton formation could be taken into account including a smooth perturbation of the dimerization order, we can approximate  $u_i^j \approx (-1)^i u^j(x)$ . The elastic interchain energies of (2) and (3) could be expanded in a gradient expansion of the lattice constant  $a$ .

$$H_{\text{el}}^{\text{sq}} = \frac{K_{\text{inter}}}{2} \sum_j \int \frac{dx}{a} (u^{j+1}(x) - u^j(x))^2 \quad (5)$$

$$H_{\text{el}}^{\text{tr}} = K_{\text{inter}} \sum_j \int \frac{dx}{a} [2u^j(x)^2 + a u^j(x) \partial_x u^{j-1}(x)] \quad (6)$$

Note that in the triangular lattice we should retain one higher order in  $a$  (the last term of (6)) to have a non-null interchain coupling. If it were not for such term the only effect of the interchain coupling would be to change the in-chain elastic coupling  $K_{\text{in}}$  by  $K_{\text{in}} + K_{\text{inter}}$ . Therefore the main effect of the interchain coupling in this case is to weaken the dimerization, reducing the magnetic gap and increasing the width of the solitons.

As in the previous analysis, a soliton could be included as point defect, thus neglecting its width. We consider that all but the 0-th chain is dimerized as the background  $u^j(x) = u_0$  for  $j \neq 0$ . For the 0-th we propose:

$$u_0(x) = u_0(-1 + \Theta(x - x_1))(-1 + \Theta(x - x_2)) \quad (7)$$

being  $\Theta(x)$  the Heaviside step function, and where we have put two solitons at positions  $x_1$  and  $x_2$  ( $x_1 < x_2$ ). By replacing in expressions (5) we obtain the interacting energy

$(4u_0^2 K_{\text{inter}}/a)(x_2 - x_1)$  which increases linearly with the distance between the solitons. Moreover using (6) the interacting energy vanishes showing the independence of the solitons.

In the previous descriptions we have neglected the interchain magnetic interaction. Moreover, we have used a point approximation for the solitons. In order to undertake a more precise study which also includes the effect of  $J_{\text{inter}}$ , we have to consider the two-chain problem, i.e. we extract a two-leg ladder from the model given in equation (1), (2) and (3). For this purpose, we have performed a numerical analysis for these models, using the DMRG finite algorithm which nowadays is accepted as the best numerical tool in low dimensional correlated systems [12]. The ladders were mapped into one-dimensional chains, where interchain interactions become next-nearest neighbour couplings. In order to avoid fictitious edge effects, we have performed the calculations with periodic boundary conditions. We have chosen 100-site ladders (50 sites each leg) to plot our results. We used the soliton width as a parameter to show that the thermodynamic limit was reached. Furthermore, this size is long enough to avoid an unwanted overlapping of possibly deconfined solitons due to their finite width. It is worth noting that when the number of sites in each leg is even, as in our case, both solitons will appear in one of the two chains. On the other hand, with an odd number of sites in each chain, one would obtain one soliton per chain but the conclusions would remain the same. We assert the reliability of the calculations keeping 200 states with a truncation error of order  $10^{-7}$ . Lattice coordinates were taken into account by solving iteratively the adiabatic equations, i.e. we take  $u_i^j$  as parameters, calculate the magnetic energy by DMRG, and minimize the total energy (magnetic + elastic) until convergence. Details of the self-consistent procedure are given elsewhere [13, 14].

From now on we set  $J_{\text{in}}$  as the energy scale and  $(J_{\text{in}}/K_{\text{in}})^{1/2}$  as the displacement one. We define the dimensionless spin-phonon coupling  $\lambda = J_{\text{in}}\alpha^2/K_{\text{in}}$ . The numerical results were obtained fixing  $\lambda = 1$  and changing  $K_{\text{inter}}$  and  $J_{\text{inter}}$ .

We start by the ground state corresponding to  $S_z = 0$ . The iterative method converge to the situation shown in figure 4. Both the square (SL) and the triangular ladders (TL) dimerize, and in the case where there is no magnetic interchain coupling, the amplitude of dimerization is smaller in the TL as previously proved.

Note that a more essential difference arises if we pay attention to the variation of the dimerization amplitude  $u_0$  with respect to  $J_{\text{inter}}$ . The variation of  $u_0$  with  $J_{\text{inter}}/J_{\text{in}}$  is shown in figure 5 for both the SL and the TL.

The dimerized state resist a stronger  $J_{\text{inter}}$  for the TL than the SL. Moreover, the dimerization amplitude is independent of  $J_{\text{inter}}$  for the TL in a wide range of this parameter. This is an important fact and implies that in the dimerized state the system remains one-dimensional even with a strong interchain coupling. A possible interpretation for this result is that each spin is paired in a singlet and in consequence the frustrated interaction cannot compete with this state until it is strong enough to break the singlet and generate an effective uniform 1D Heisenberg model along the

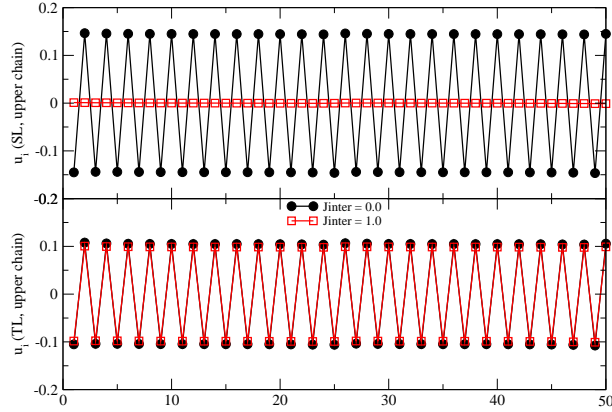


**Figure 4.** Lattice distortion in the dimerized state corresponding to the  $S_z = 0$  subspace for: (a) square and (b) triangular ladders. As the distortions in both chains are the same we only show results for the upper one. We have fixed  $K_{\text{inter}}/K_{\text{in}} = 0.5$ .

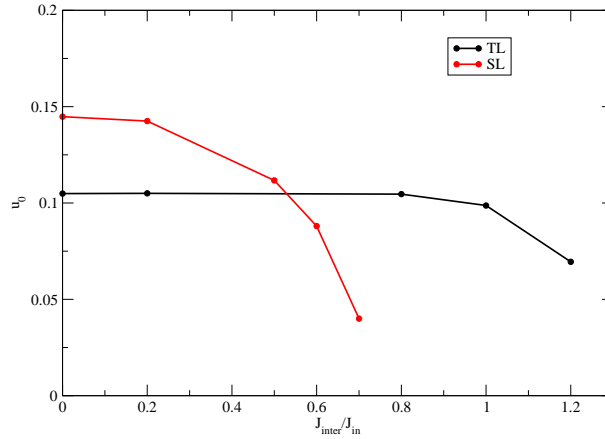


**Figure 5.** Dimerization amplitude as a function of  $J_{\text{inter}}/J_{\text{in}}$  for the SL and the TL. Again we use the same elastic parameter indicated in the caption of figure 4.

zig-zag path.

Now let us analyze the excited state. In figure 6 and 7 we show the lattice deformation and the local magnetization for the square ladder.

There are two defects of the dimerization pattern. Distortions far away from that defects correspond to the dimerization pattern with the same value as in figure 4 ( $u_0 = 0.15$ ). The defect cannot be considered as two independent solitons because they always fall at the same distance independently of the initial distortion pattern used in the method. The deformation of the intermediate region between the defects does not correspond to the dimerization of the bulk and correspondingly  $\langle S_{zi} \rangle$  does not vanish in this intermediate zone. Therefore we fail to describe this pattern as a two-soliton form that would be given by

$$u_i = (-1)^i u_0 \tanh\left(\frac{i - x_1}{\xi}\right) \tanh\left(\frac{i - x_2}{\xi}\right) \quad (8)$$

where  $\xi$  is the soliton width. It is better described as the domain excitation found



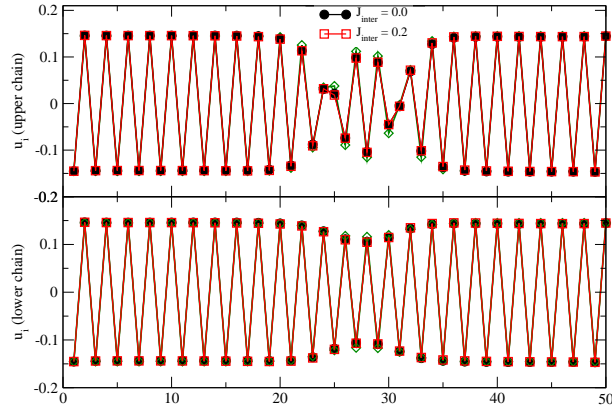


**Figure 6.** Lattice distortion for the upper and lower chains of the SL in the  $S_z = 1$  subspace. The green curve is a fitting to the analytic result given by equations (9) and (10).

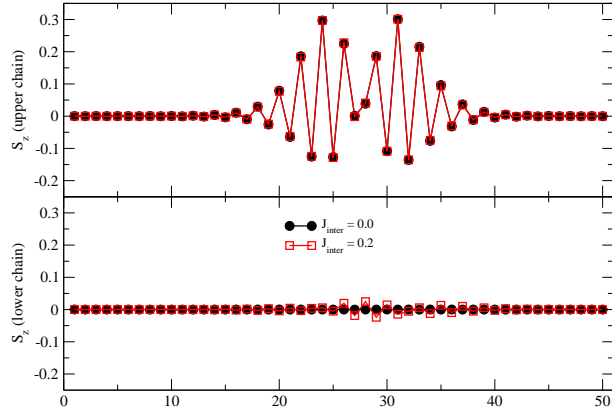


**Figure 7.** Local magnetization for the upper and lower chains of the square ladder in the subspace  $S_z = 1$ .

in [6] for the square lattice. It was obtained by bosonization techniques and the self-consistent harmonic approximation (SCHA). For comparison, we redo the calculation of [6] for the two-chain spin-phonon system coupled by an elastic interaction. To solve the SCHA equations we fix the bosonic field representing the spin variables in one of the chains (say 1) to its value in the  $S_z = 0$  dimerized state [6]. The displacement fields  $u_1(x) = (-1)^i u_i^1$  and  $u_2(x) = (-1)^i u_i^2$  are then given by the following expressions:

$$u_1(x) = \frac{u_0}{\frac{\epsilon}{2} + 1} \left[ \left(1 + \frac{\epsilon}{4}\right) + \frac{\epsilon}{4} t(x - x_M) \right] \quad (9)$$

$$u_2(x) = \frac{u_0}{\frac{\epsilon}{2} + 1} \left[ \frac{\epsilon}{4} + \left(1 + \frac{\epsilon}{4}\right) t(x - x_M) \right] \quad (10)$$

where  $\epsilon = K_{\text{inter}}/K_{\text{in}}$ ,  $x_M$  sets the position of the domain in the chain 2 and the function  $t(x)$  is given by:

$$t(x) = 1 - 2 \cosh^2(x_0/\xi) \times \operatorname{sech} \left[ \frac{(x - x_0)}{\xi} \right] \operatorname{sech} \left[ \frac{(x + x_0)}{\xi} \right] \quad (11)$$

with:

$$\frac{x_0}{\xi} = \frac{1}{2} \log \left[ \frac{2 + B + 2\sqrt{1+B}}{B} \right], \quad B = \frac{1}{1 + \frac{4}{\epsilon}} \quad (12)$$

being  $\xi$  a characteristic width of the wall of the domain.  $2x_0$  measures the 'radius' of the domain configuration. Note that for each interchain coupling  $\epsilon$ ,  $x_0$  is fixed by equation (12), i.e. the wall of the domain accommodates at a given equilibrium distance. Only for negligible values of  $\epsilon$  the domain dissociate in two separate domain walls as given in equation 8. For any finite  $\epsilon$ , the walls are as close as they can in order to reduce the interchain energy.

An accurate fitting could be found between the DMRG results and the analytic form given in equation (10). Lines in figure 6 were obtained from this equation with  $\xi = 1.84$  and  $x_M = 27.71$ .  $x_0/\xi = 1.82$  has not been taken as a fitted parameter but obtained from equation (12). The slight reduction of the dimerization in the lower chain is well predicted by the analytic expression in equation (9). With the same values for the parameters a very good agreement is found as shown in the lower panel of figure 6. The overall coincidence prove that the spin-1 excitation we found numerically could be identified with the domain predicted in analytic calculations based on bosonization.

On the other hand, we also study the effect of a magnetic interchain coupling ( $J_{\text{inter}}/J_{\text{in}} = 0.2$ ). The only perturbation is a small magnetic polarization of the lower chain debilitating the singlets in this chain as observed in figure 7. The displacements  $u_i$  do not change with the presence of  $J_{\text{inter}}$ , and the distortions are shown in figure 6.

A quite different situation occurs in the triangular ladder. In this case the two defects appear separate enough to give the possibility that the intermediate zone dimerizes as the bulk. The situation is shown in figure 8. The two defects of the

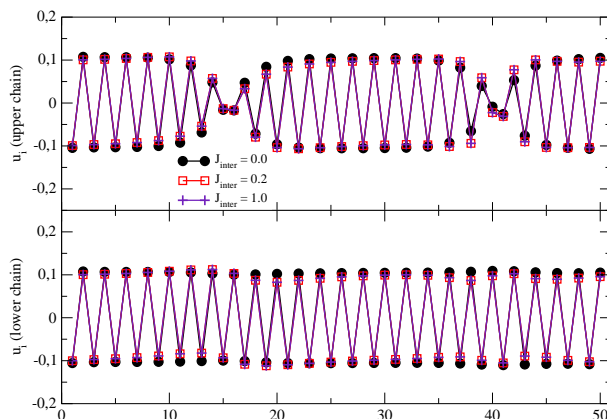


**Figure 8.** Lattice distortion for the upper and lower chains of the TL in the subspace  $S_z = 1$ .

dimerization order are now far apart. The deformation pattern can now be fitted by a two-soliton function as given in equation (8). For the set of parameters we used, we have found a soliton width of  $\xi \simeq 3.096$ . Different runs give patterns like those of figure 8 but the distance between the solitons  $x_2 - x_1$  depends on the initial distortion

pattern. As our method minimizes the total energy this is an indication that solitons are independent excitations.

Let us analyze the effect of the magnetic interchain coupling. As a soliton could be thought as a free spin in a background of singlets it is expected that a weak  $J_{\text{inter}}$  should not have much influence in the soliton formation and their interactions. This is in fact the case for  $J_{\text{inter}}/J_{\text{in}} = 0.2$  as shown in figure 9. It is interesting to remark that even

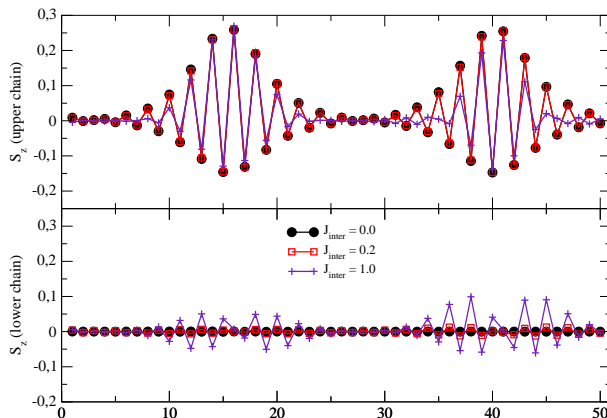


**Figure 9.** Local magnetization for the upper and lower chains of the TL in the subspace  $S_z = 1$ .

when the interchain coupling equals the in-chain one the basic physics does not change. The distortion pattern is described by a two-soliton function and the local magnetization of the upper chain increase but the perturbation remains localized. Therefore we predict that independent solitons could be the elementary excitations even in this case.

Until now we have found the lattice deformation by minimizing the total energy of the system. Now we take the solitons as elementary entities and analyze the question of their interaction energy. Once the distortions have been fitted by the function (8) we modify the distance between the solitons changing the values of  $x_2 - x_1$ . We calculate the total energy as a function of the distance  $d = x_2 - x_1$ . Results are shown in figure 10. We have subtracted the energy of the dimerized state in order to obtain the creation energy of the solitons plus their interaction energy. The energy increases at small distances. This effect could be interpreted as a repulsion between the solitons when their distance is smaller than twice their width. For larger separations the energy does not depend on the distance. This fact shows that solitons are indeed independent when they are far apart. The inclusion of a  $J_{\text{inter}} = 0.2$  does not modify this picture as shown in the figure 10.

The role of the interchain coupling frustration in stabilizing deconfined spinons was recently discussed in purely magnetic coupled chains by Nersesyan and Tsvelik [15]. To make contact with this study we should consider our spin-phonon model beyond the adiabatic approximation. Actually the partition function of the model given by equations (1) and (3) could be formulated as a path integral. Moreover, the lattice

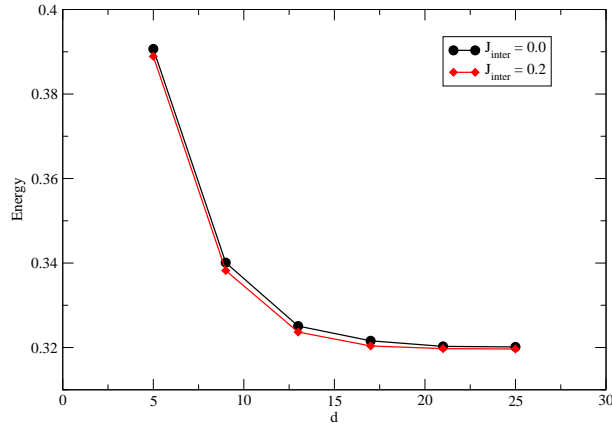


**Figure 10.** Dependence of the interaction energy with the distance between two solitons, for the triangular ladder.

coordinates  $u_i$  could be integrated out producing a retarded interaction between the spin variables. In the antiadiabatic limit this interaction becomes instantaneous. The effective magnetic model will contain, in addition to the original interchain magnetic interactions, four-spin exchange interactions as the one included in previous models leading to deconfined spinons [16, 17, 18]. It would be very interesting to study the spin-phonon model by the techniques used in [16, 17] to analyze the appearance of deconfined spinons when the phonon dynamics is included. On a general ground we could assert that the deconfined scenario discussed in the present paper is connected with a local symmetry transformation that acts on each individual chain changing one of the two possible dimerized states into the other one. This emergent  $Z_2$  gauge symmetry is at the heart of the deconfinement mechanism found in the magnetic model in [18]. Therefore, we expect the appearance of a deconfined quantum critical point in this model as found previously in the simplest spin system.

Note the differences with the model of spin-phonon chains coupled by non-frustrated interactions. This model could be mapped into an effective Ising model of coupled chains [19]. The mapping takes into account the underlying *global*  $Z_2$  symmetry of the dimer order parameter. The symmetry is spontaneously broken in the low temperature phase and the solitons are confined. In the frustrated case the dimerization phases between different chains are uncorrelated and the mapping of Ref. [19] leads to decoupled Ising chains which is a manifestation of the deconfinement of solitons discussed in the present paper.

Let us finish with the following remark. As previously discussed, in order to fix the dimerization order in the direction perpendicular to the magnetic chains, we should add a next-nearest neighbour elastic interaction. Analogously to the argument used for the square geometry, this effect will provide a confinement mechanism for the solitons. Even though this coupling might be necessary to modelize the compounds TiOCl and TiOBr, the results of the present paper could be the starting point to describe the spectrum at not too low temperatures, i.e. above the point where the elastic next-nearest neighbour

energy starts to be washed out by the thermal energy.

In summary, we have shown an essential difference in the ground state and the elementary excitations of coupled spin-Peierls chains depending on the nature of the interchain coupling, i.e. with and without frustration. In the frustrated case we have found that the amplitude of dimerization in the ground state is independent of the strength of the magnetic interchain coupling in a broad range of values of the parameter  $J_{\text{inter}}$ . Moreover, the analysis of the elementary excitations showed that solitons of the individual chains survive the inclusion of a nearest-neighbour interchain coupling. As our approach relies in a static approximation of the phonon field we cannot make precise predictions on the dynamical response of the system. On a general ground we can speculate that a two-soliton continuum should appear in the frustrated system. This is a different behaviour than that measured in a non-frustrated spin-Peierls system.

## Acknowledgments

We thank D. Cabra for helpful discussions. This work was partially supported by PIP CONICET (Grant 5036).

## References

- [1] Tennant D A, Cowley R A, Nagler S E and Tsvelik A M 1995 *Phys. Rev. B* **52** 13368
- [2] Coldea R, Tennant D A, Tsvelik A M and Tyliczynski 2001 *Z Phys. Rev. Lett.* **86** 1335
- [3] Nakano T and Fukuyama H 1980 *J. Phys. Soc. Japan* **49** 1679
- [4] Augier D, Poilblanc D, Sorensen E and Affleck I 1998 *Phys. Rev. B* **58** 9110
- [5] Affleck I 1997 *Dynamical Properties of Unconventional Magnetic Systems* NATO Advanced Study Institute, Series B:Physics, Norway (Plenum, New York)
- [6] Dobry A and Ibaceta D 1998 *Phys. Rev. B* **58** 3124
- [7] Essler F H L, Tsvelik A M and Delfino G 1997 *Phys. Rev. B* **56** 11001
- [8] Citro R, Orignac E and Giamarchi T 2005 *Phys. Rev. B* **72** 24434
- [9] Aïm M, Lorenzo J E, Regnault L P, Dhahenne G, Revcolevschi A, Hennion B and Jolicoeur Th 1997 *Phys. Rev. Lett.* **78** 1560
- [10] Seidel A, Marianetti C A, Chou F C, Ceder G and Lee P A 2003 *Phys. Rev. B* **67** 020405(R)
- [11] Rückamp R, Baier J, Kriener M, Haverkort M W, Lorenz T, Uhrig G S, Jongen L, Möller A, Meyer G and Grüninger M 2005 *Phys. Rev. Lett.* **95** 097203
- [12] Schollwöck U 2005 *Rev. Mod. Phys.* **77** 259; Hallberg K 2006 *Advances in Physics* **55** 477
- [13] Feiguin A E, Riera J A, Dobry A and Ceccatto H A 1997 *Phys. Rev. B* **56** 14607
- [14] Vekua T, Cabra D C, Dobry A, Gazza C and Poilblanc D 2006 *Phys. Rev. Lett.* **96** 117205
- [15] Nersesyan A A and Tsvelik A M 2006 *Phys. Rev. B* **67** 024422
- [16] Tsvelik A M 2004 *Phys. Rev. B* **70** 134412
- [17] Starykh O A and Balents L 2004 *Phys. Rev. Lett.* **93** 127202
- [18] Batista C D and Trugman S A 2004 *Phys. Rev. Lett.* **93** 217202
- [19] Mostovoy M and Khomskii D 1997 *Z. Phys. B* **103** 209